scientific reports

Check for updates

OPEN

Ab initio determination on diffusion coefficient and viscosity of FeNi fluid under Earth's core condition

Wei-Jie Li[1✉], Zi Li[2,3], Zhe Ma[1], Ping Zhang[2,3,4], Yong Lu[5], Cong Wang[2,3,4✉], Qian Jia[6], Xue-Bin Cheng[1] & Han-Dong Hu[1]

The Earth's outer core is mainly composed of Fe and Ni. The geodynamo of the Earth's core are closely correlated with the transport properties of the fluid in the Earth's core. We selected the typical FeNi fluid, and systemically calculated its diffusion coefficient and viscosity under Earth's core condition by quantum molecular dynamics simulation. The diffusion coefficients are almost constant along the core adiabatic curve. The self-diffusion coefficients of Ni along the core adiabatic curve range from 2.47×10^{-9} to 3.37×10^{-9} m^2s^{-1}. The diffusion coefficient increases with temperature increase, while viscosity decrease with temperature increase. The calculations on the transport properties suggest that the Ni impurities have a negligible effect on the diffusion coefficient and viscosity of Earth's core.

Accurate knowledge of the physical properties under extreme pressure–temperature conditions is of considerable interest in various fields of physics, including the Earth system[1], planetary physics[2], astrophysics[3], and inertial confinement fusion[4]. The center of the Earth consists of a solid inner core, surrounded by a spherical shell of the liquid outer core. The vigorous convection in the metallic liquid outer core thus powers the dynamo that sustains the magnetic field. The geodynamo is extremely sensitive to core conditions, which is a very active research topic in Earth science. The viscosity and diffusion coefficients of the Earth's core are the main parameters in the convection process.

In the early reported paper[5], the diffusion coefficient in the diffusion equation is mostly adopted as 3×10^{-9} m^2s^{-1}. It is difficult to get the accurate diffusion coefficient and viscosity values under Earth's core condition experimentally[6]. Now, quantum molecular dynamics (QMD) can give a direct and quantitative estimation of the transport coefficients[7]. The QMD results show that the self-diffusion coefficient of Fe is 5.2×10^{-9} m^2/s, and viscosity is 8.5 mPa s at T = 4300 K and density ρ = 10,700 kg m^{-3}[8]. Recently, light element effects on transport properties were also considered, such as Fe–Si–O fluid[9], Fe–O fluid[10,11], Fe–S fluid[12].

The QMD results of viscosity are far lower than the values inferred from seismic and other measurements[13,14]. Early in 1998, it was inferred that the viscosity of the inner core is 1.22×10^{11} Pa s[15]. Geodynamic estimation by Buffett inferred viscosity is less than 10^{16} Pa s[16]. The theoretical value for viscosity varies largely by different methods, from ~ 1 mPa s[14,17] under the outer condition to 10^{11} Pa s[15] under the inner core condition. QMD calculation shows that the viscosity is 13 mPa s and diffusion coefficients 5×10^{-9} m^2s^{-1} at the inner-core boundary(ICB), and 12 mPa and 4×10^{-9} m^2s^{-1} at the core-mantle boundary (CMB)[18]. The viscosity is about several mPa s for MD results of FeNi fluid[19]. Though there were limitations in MD, the early reported MD results claim that Ni has a negligible effect on viscosity[17]. However, the MD results dependent on the empirical parameters of atom potential, and the self-diffusion coefficient of Fe and Ni are not fully reported. AIMD is an optimal method for the calculation of ionic transport properties without empirical parameters.

However, the self-diffusion coefficient and viscosity of Fe–Ni fluid at Earth's core condition have never been calculated by QMD. In this paper, we calculated the diffusion coefficients and viscosity of Fe–Ni fluid under Earth's core condition by the precisely QMD methods, and give a simple analysis of the temperature effect on transport properties of Fe–Ni fluid.

[1]Intelligent Science and Technology, Academy Limited of CASIC, Beijing 100144, People's Republic of China. [2]Institute of Applied Physics and Computational Mathematics, Beijing 100088, People's Republic of China. [3]Tianfu Innovation Energy Establishment, Chengdu 610213, China. [4]Center for Applied Physics and Technology, Peking University, Beijing 100871, People's Republic of China. [5]College of Mathematics and Physics, Beijing University of Chemical Technology, Beijing 100029, China. [6]X LAB, The Second Academy of CASIC, Beijing 100854, People's Republic of China. ✉email: liweijie8680@126.com; wang_cong@iapcm.ac.cn

Methods and calculations

Transport property. The theory equations are collected from Ref.[7,20–22]. Diffusion coefficients can be calculated by either velocity autocorrelation functions or mean-squared displacements by equilibrium molecular simulation. The self-diffusion coefficient D_i of element i is calculated by the Einstein equation from velocity correlation function $A(t)$ is

$$A(t) = \langle \mathbf{V}_i(t)\mathbf{V}_i(0) \rangle,$$
$$D_i = \frac{1}{3} \int_0^\infty A(\tau)d\tau, \tag{1}$$

where $V_i(t)$ is the velocity of species i at time t. and $<\dots>$ is an average of velocity correlation function over atoms. From the sight of mean square displacement (MSD) $M(t)$, D_i is the asymptotic slope of $M(t)$ as a function of time:

$$M(t) = \frac{1}{N_I} \sum_{N_I} \left\langle |\mathbf{R}_i(t) - \mathbf{R}_i(0)|^2 \right\rangle,$$
$$D_i = \lim_{t\to\infty} \frac{M(t)}{6t}, \tag{2}$$

where $R_i(t)$ is the trajectory of a species atom i, and N_I is the number of ions.

Calculated by the Green–Kubo relation, the shear viscosity η is the integral of the autocorrelation function of the off-diagonal component of the stress tensor (ACF) $S(t)$.

$$C_{\alpha\beta}(t) = \left\langle P_{\alpha\beta}(t + t_0)P_{\alpha\beta}(t_0) \right\rangle$$
$$\eta = \frac{V}{k_B T} \lim_{t\to\infty} \int_0^t S(t')dt'$$
$$S(t) = \frac{1}{5}\left\{ C_{xy}(t) + C_{yz}(t) + C_{zx}(t) + \frac{1}{2}\left[C_{xx}(t) - C_{yy}(t)\right] + \frac{1}{2}\left[C_{yy}(t) - C_{zz}(t)\right] \right\} \tag{3}$$

where k_B is the Boltzmann factor, T is temperature and V is the volume of the cell. The results are averaged from the five independent off-diagonal components of the stress tensor P_{xy}, P_{yz}, P_{zx}, $(P_{xx}–P_{yy})/2$, and $(P_{yy}–P_{zz})/2$. We adopt empirical fits to the integrals of the autocorrelation function. Both D_i and η have been fit to the function in the form of $A\left[1 - exp(-t/\tau)\right]$, where A and τ are free parameters. The fractional statistical error in calculating a correlation function C for molecular dynamics trajectories[23] can be given by

$$\frac{\Delta C}{C} = \sqrt{\frac{2\tau}{T_{traj}}}, \tag{4}$$

where T_{traj} is the length of the trajectory and τ is the correlation time of the function. In the present paper, we generally fitted over a time interval of $[0,4\tau–5\tau]$.

The pair correlation function (PCF) $g(r)$ or radial distribution function is usually used to describe quantitatively the internal structure of fluids.

$$g(r) = \frac{V}{4\pi r^2 N^2} \left(\sum_i \sum_{j\neq i} \delta\left(r - r_{ij}\right) \right) \tag{5}$$

where r is radius distance, r_{ij} and N is atom number. The PCF quantifies how the particle of interest is surrounded by other particles.

Calculation details. Ab initio molecular dynamics were performed using the Vienna ab initio simulation package (VASP)[24,25]. The ion–electron interaction was represented by the projector augmented wave (PAW)[26,27]. The generalized gradient approximation with Perdew, Burke, and Ernzerhof corrections was employed[28]. The electronic states were populated following the Fermi–Dirac distribution[29]. For the convergence of transport property values, the size of the system is checked. Herein, 128 atoms are selected as the cell. Ni atoms were randomly distributed in the cell, with 12 Ni atoms and others are Fe atoms, and the corresponding atom ratio are 9.375 at.%. Plane wave cutoff is 400 eV enough to make sure that the pressure is converged within 1% accuracy. Time dependent mean square displacement was checked to make sure that the system is in a liquid state. The selected time step is 1 fs in all the calculations. To get the convergent transport coefficients, the total time is more than 20 ps with the beginning 2 ps discarded for equilibration. The core-mantle boundary (CMB) pressure is 136 GPa, inner-core boundary (ICB) pressure is 330 GPa, and pressures under outer core conditions were selected, such as 150 GPa, 200 GPa, 250 GPa, 300 GPa. The analytical expressions of the pressure and temperature profiles along the adiabatic curve were given by following Labrosse[30].

It is assumed that the Earth's outer core is in a well-mixed state with an adiabatic pressure–temperature profiles. The temperature and pressure profiles is the same as reported in[30]. The pressure P at radius (r) is
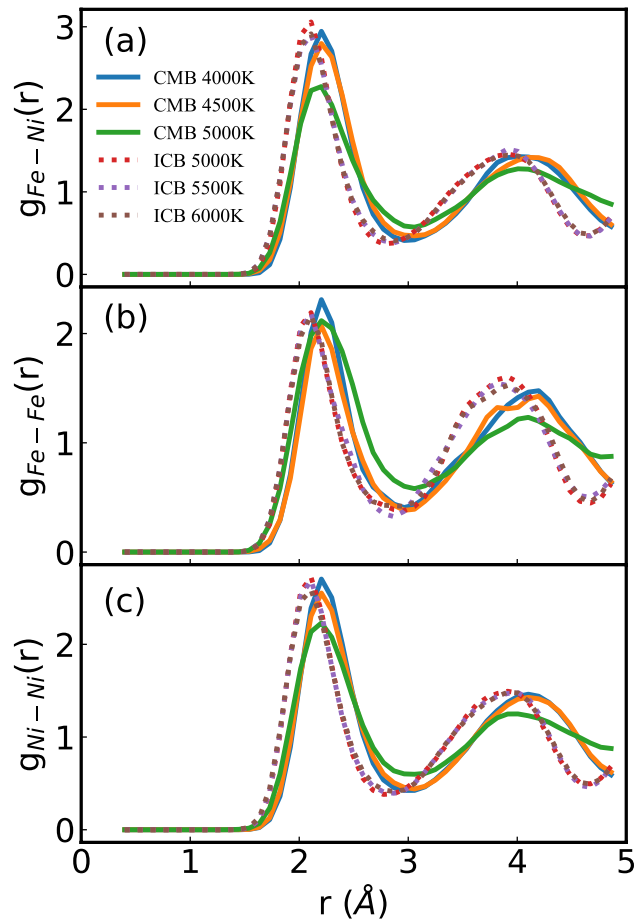
Figure 1. Pair correlation functions of (**a**) Fe–Ni ($g_{Fe-Ni}(r)$), (**b**) Fe–Fe ($g_{Fe-Fe}(r)$) and (**c**) Ni–Ni ($g_{Ni-Ni}(r)$) in FeNi fluid under Earth's core condition. The label 'ICB' and 'CMB' represent pressure at 330 GPa and 136 GPa, respectively.

$$P(r) = P_c + \frac{4\pi G \rho_{cen}^2}{3} \left[\left(\frac{3r^2}{10} - \frac{L^2}{5} \right) \exp\left(-\frac{r^2}{L^2} \right) \right]_r^{r_c} \tag{6}$$

where P_c and ρ_{cen} are the pressure and density at the center of Earth, respectively; G is the Gravitational constant; L is the lengthscale; and r_c is the radius at the CMB. $G = 6.6873 \times 10^{-11}$ m^{3}kg^{-1} s^{-2}, $L = 7272$ km, and $r_c = 3480$ km. With the $P(r_c) = 136$ GPa and $P(r_i) = 330$ GPa, the pressures $P(r)$ in the outer core are collected.

The adiabatic temperature T_a at radius r is

$$T_a(r) = T_{cen} \exp\left(-\frac{r^2}{D_L^2} \right) \tag{7}$$

where T_{cen} is the temperature at the center of the Earth, and D is the lengthscale. $T_{cen} = 5726$ K, and $D_L = 6203$ km.

Results and discussion

Ab initio calculated results. After getting the equilibrium information of the QMD, the pair correlation function $g(t)$ (Fig. 1), mean-square displacement $M(t)$ (Fig. 2a), and autocorrelation function of the off-diagonal component of the stress tensor $S(t)$ (Fig. 2b) can be calculated. The shape of $g(r)$ and $M(t)$ of FeNi fluid is similar to early reported results[13], and the calculated FeNi fluid is a close-packed liquid. The g(r) shapes of Fe–Ni, Fe–Fe, and Ni–Ni are similar, which implied that Fe and Ni atoms are similarly distributed. The $g(r)$ tends towards a uniform value of 1 for a large value of r. The first peak location of $g(r)$ at ICB is closer to the zero point than at CMB. From the QMD results, the equilibrium volume of Fe–Ni fluid is 8.274 Å^3/atom at CMB and 4000 K and 6.933 Å^3/atom at ICB and 5500 K, respectively. The $g(r)$ results are consistent with the QMD calculated equilibrium volume. The peaks of $g(r)$ decrease with temperature increase, especially at CMB conditions, which indicated that $g(r)$ at high temperature easily converged to unity.

The mean-square displacement $M(t)$ of Fe and Ni becomes a linear function of time after sufficiently large random steps (Fig. 2a). As the mobility of Fe and Ni are similar, only $M(t)$ of Fe is plotted in Fig. 2a. The diffusive regime ($\sim t^1$) gives a self-diffusion coefficient which starts after a ballistic period of dozens of fs. At 136 GPa or
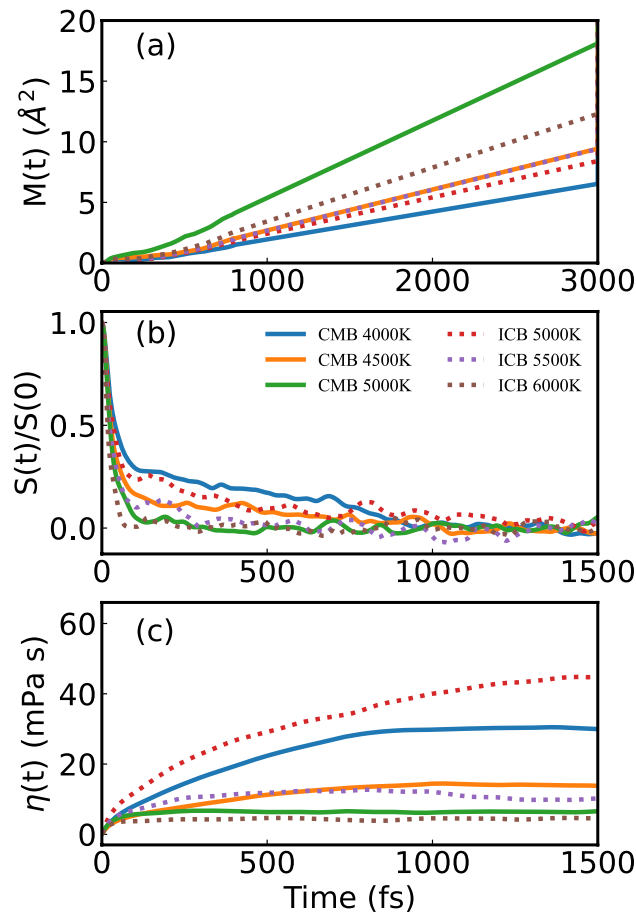
Figure 2. (**a**) Mean squared displacements of Fe–Fe M(t), (**b**) autocorrelation function of traceless stress tensor S(t) and (**c**) time evoluted viscosity η(t) in FeNi fluid under Earth's core condition. The label 'ICB' and 'CMB' represent 330 GPa and 136 GPa, respectively. The S(0) is velocity-velocity autocorrelation function at t = 0.

330 GPa, the *M(t)* increases nonlinearly with temperature increase. The self-diffusion coefficient is the slope of *M(t)*, it confirmed that the self-diffusion coefficient increases with the increase of temperature. The shape of *S(t)*, and *η(t)* is the same as reported[31] (Fig. 2b–c). The *S(t)* goes to zero as time tends to infinity. The present ACF at CMB in Fig. 2 looks to decay slower than that reported data at CMB in Ref.[8]. Not only the temperature and pressure states are different from[8], but also the thermostats in our calculation are different. The ACF convergence time and behavior may be different from previous work. The error is estimated with the analytic expression in Eq.(1). At 136 GPa or 330 GPa, the *η(t→0)* decreases with the increase of temperature. Then, the viscosity of FeNi fluid decreases with the temperature.

Self-diffusion coefficient. Our QMD calculations on the self-diffusion coefficient of pure Fe liquid are lower than the early reported QMD results[8,9,18] (Fig. 3a). The main difference is that the adiabatic temperatures in this calculation are lower than the reported results. From Fig. 3b, the temperature effect on the self-diffusion coefficient exhibit Arrhenius behaviors, and self-diffusion coefficients of Fe and Ni increase with the increase of temperature. Then, it is reasonable that the self-diffusion coefficient of Fe in this manuscript is a bit lower than reported in Refs.[8,9,18]. The self-diffusion coefficients of Fe and Ni are comparable, in the orders of 10^{-9} m^2s^{-1}. Our calculated self-diffusion coefficients of Fe are consistent with the ab initio calculated results of pure Fe[8], Fe–Si–O fluid[9], and Fe–O fluid[11].

Self-diffusion coefficients of Fe along the core adiabatic are in the range of $[2.58, 3.35] \times 10^{-9}$ m^2s^{-1}. Self-diffusion coefficients of Ni along the core adiabatic are in the range of $[2.47, 3.37] \times 10^{-9}$ m^2s^{-1}. The self-diffusion coefficient of Fe–Ni fluid along the core adiabatic is almost constant (Fig. 3a and Table 1). The self-diffusion of Ni is a little smaller than that of Fe at the same pressure and temperature condition. From one sight, the atom mass of Ni is a little higher than that of Fe, which shows that the self-diffusion coefficient of Ni and Fe are similar, but Ni atoms move slower than Fe atoms. Considering the pressure and temperature effect (Fig. 3b), the self-diffusion coefficient is higher when at the same pressure with a higher temperature or the same temperature with lower pressure. The temperature and pressure effect on the self-diffusion coefficient in FeNi fluid can also be obtained by analyzing the of mean squared displacement (Fig. 2). Self-diffusion coefficient of Fe at CMB ranges from
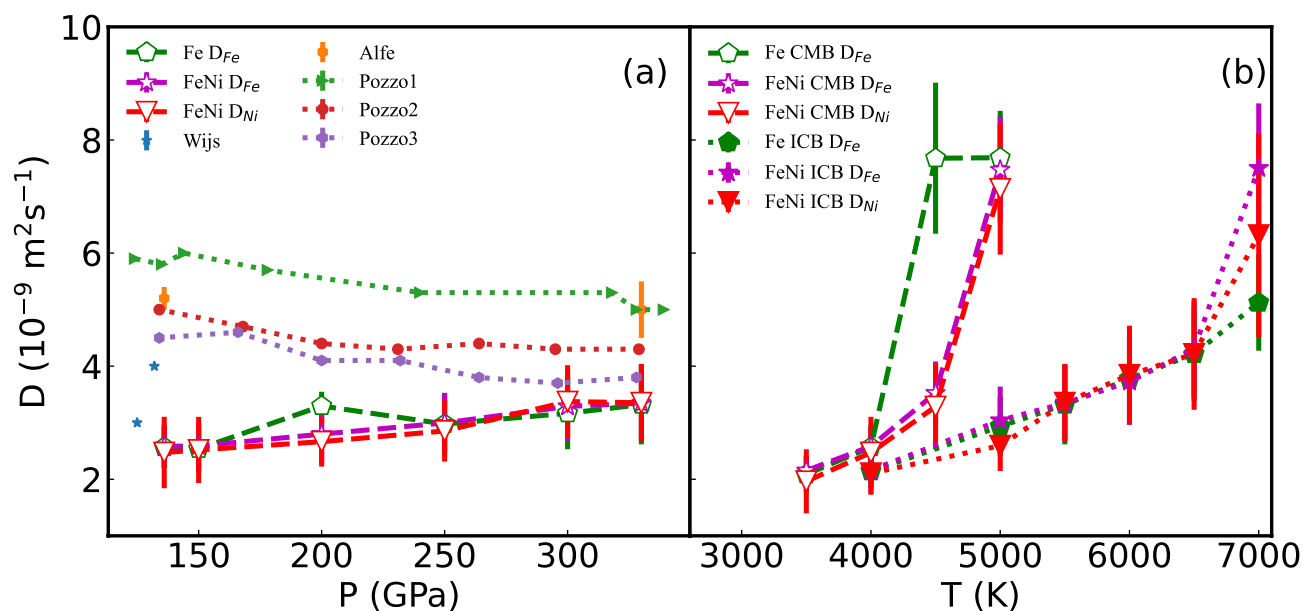
Figure 3. The self-diffusion coefficients (D_{Fe} and D_{Ni}) of Fe and FeNi fluid under Earth's core conditions. (**a**) is along the core adiabatic, and (**b**) is temperature variation at CMB and ICB. 'Wijs'[18], 'Alfe'[8], 'Pozzo1'[9], 'Pozzo2'[9] and 'Pozzo3'[9] represent the self-diffusion coefficient of Fe in Fe, $Fe_{0.82}Si_{0.10}O_{0.08}$ and $Fe_{0.79}Si_{0.08}O_{0.13}$ fluids.

| Pressure (P, GPa)	Temperature (T, K)	Equlibrium volume per atom (Å³)	Self-diffusion coefficient of Fe (D_{Fe}, 10^{-9} m²s⁻¹)	Standard error of D_{Fe} (δD_{Fe} 10^{-9} m²s⁻¹)	Self-diffusion coefficient of Ni (D_{Ni}, 10^{-9} m²s⁻¹)	Standard error of D_{Ni} (δD_{Ni} 10^{-9} m²s⁻¹)	Viscosity (η, mPa s)	Standard error of η ($\delta\eta$, mPa s)
136	3944	8.27	2.58	0.38	2.47	0.63	29.95	5.50
150	4057	8.14	2.59	0.41	2.52	0.59	23.43	5.35
200	4460	7.70	2.80	0.53	2.67	0.44	26.93	4.32
250	4863	7.36	3.00	0.52	2.85	0.54	8.55	1.44
300	5265	7.08	3.29	0.61	3.37	0.64	7.88	0.73
330	5507	6.93	3.35	0.67	3.35	0.69	12.09	1.34

Table 1. Self-diffusion coefficient and viscosity of FeNi fluid along the core adiabatic curve.

$(2.15 \pm 0.26) \times 10^{-9}$ at 3500 K to $(7.47 \pm 0.94) \times 10^{-9}$ m²s⁻¹ at 5000 K. The self-diffusion coefficient of Ni at CMB ranges from $(1.96 \pm 0.57) \times 10^{-9}$ at 3500 K to $(7.14 \pm 1.16) \times 10^{-9}$ at 5000 K.

Shear viscosity. The viscosity of FeNi fluid along the adiabatic curve is in the range of [7.78, 29.95] mPa s, and the viscosity of Fe fluid is in the range of [10.10, 22.51] mPa s (shown in Fig. 4a). The viscosity of Fe-10%Ni fluid is higher than pure Fe, under ICB, and CMB (Fig. 4b). The QMD result is different from the early reported MD results[17], which point out Ni has a negligible effect on bulk viscosity of liquid iron, about ~ mPa s[17]. Furthermore, the QMD results of viscosity are far lower than the values inferred from seismic and other measurements[13,14], and higher than those calculated by MD[17]. The viscosity near the CMB condition reported in this manuscript is higher than the reported results by Pozzo at the same condition (Fig. 4a). The adiabatic temperature in this calculation is lower than Ref.[9]. At 136 GPa or 330 GPa, the viscosity decreases as the increase of temperature (Fig. 4b). Temperature effect on shear viscosity exhibit Arrhenius behaviors. Then, a slightly low temperature also corresponds to a high viscosity at the same pressure, and the temperature effect is obvious when at a slightly low temperature.

Conclusion

Ab initio molecular dynamics estimates self-diffusion coefficient and viscosity of outer core are important for several purposes. The pair correlation function, mean square displacement, and autocorrelation function of trace-less stress tensor are analyzed by the ab initio calculated equilibrium information. Self-diffusion coefficients of Ni along the core adiabatic range from 2.47×10^{-9} to 3.37×10^{-9} m²s⁻¹. The viscosity of FeNi fluid along the core adiabatic range from 7.88 to 29.95 mPa s. At the core-mantle boundary, the diffusion coefficient increases with temperature increase, while viscosity decrease with temperature increase as expected.
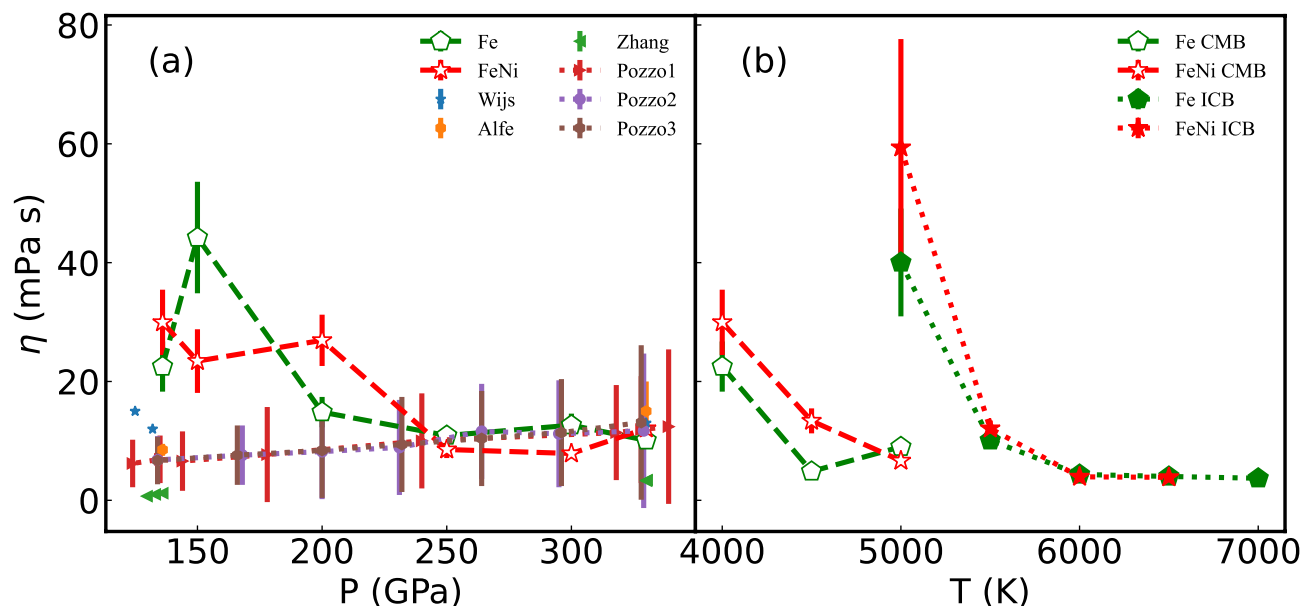
Figure 4. Viscosity of the pure Fe and FeNi fluid under Earth's core condition. (**a**) is viscosity along the adiabatic curve and (**b**) is viscosity under inner-core (136 GPa) and core-mantle (330 GPa) boundary pressure with different temperatures. The Fe and FeNi labels correspond to pure Fe and FeNi fluid results, respectively.

Data availability

The data that support the findings of this study are available from the corresponding authors upon reasonable request.

References

1. Mao, H.-K. & Mao, W. L. Key problems of the four-dimensional earth system. *Matter Radiat. Extrem.* **5**, 038102 (2020).
2. Lorenzen, W., Becker, A. & Redmer, R. *Frontiers and Challenges in Warm Dense Matter 203–234* (Springer, Cham, 2014).
3. Saumon, D., Chabrier, G. & Van Horn, H. An equation of state for low-mass stars and giant planets. *Astrophys. J. Suppl. Ser.* **99**, 713 (1995).
4. Yamanaka, C. Inertial confinement fusion: The quest for ignition and energy gain using indirect drive. *Nucl. Fusion* **39**(6), 825 (1999).
5. Buffett, B. A. & Seagle, C. T. Stratification of the top of the core due to chemical interactions with the mantle. *J. Geophys. Res. Solid Earth* **115**(B4), (2010).
6. Dobson, D. P. Self-diffusion in liquid Fe at high pressure. *Phys. Earth Planet. Inter.* **130**, 271–284 (2002).
7. Wang, C., Wang, Z.-B., Chen, Q.-F. & Zhang, P. Quantum molecular dynamics study of warm dense iron. *Phys. Rev. E* **89**, 023101 (2014).
8. Alfè, D., Kresse, G. & Gillan, M. Structure and dynamics of liquid iron under Earth's core conditions. *Phys. Rev. B* **61**, 132 (2000).
9. Pozzo, M., Davies, C., Gubbins, D. & Alfè, D. Transport properties for liquid silicon-oxygen-iron mixtures at Earth's core conditions. *Phys. Rev. B* **87**, 014110. https://doi.org/10.1103/PhysRevB.87.014110 (2013).
10. Gubbins, D. & Davies, C. The stratified layer at the core–mantle boundary caused by barodiffusion of oxygen, sulphur and silicon. *Phys. Earth Planet. Inter.* **215**, 21–28 (2013).
11. Ichikawa, H. & Tsuchiya, T. Atomic transport property of Fe–O liquid alloys in the Earth's outer core P, T condition. *Phys. Earth Planet. Inter.* **247**, 27–35 (2015).
12. Vočadlo, L., Alfè, D., Price, G. D. & Gillan, M. J. First principles calculations on the diffusivity and viscosity of liquid Fe-S at experimentally accessible conditions. *Phys. Earth Planet. Inter.* **120**, 145–152. https://doi.org/10.1016/S0031-9201(00)00151-5 (2000).
13. Vočadlo, L., de Wijs, G. A., Kresse, G., Gillan, M. & Price, G. D. First principles calculations on crystalline and liquid iron at Earth's core conditions. *Faraday Discuss.* **106**, 205–218 (1997).
14. Su, W.-J., Dziewonski, A. M. & Jeanloz, R. Planet within a planet: Rotation of the inner core of Earth. *Science* **274**, 1883–1887 (1996).
15. Smylie, D. E. Viscosity near earth: Solid inner core. *Science* **284**, 461. https://doi.org/10.1126/science.284.5413.461 (1999).
16. Buffett, B. A. Geodynamic estimates of the viscosity of the Earth's inner core. *Nature* **388**, 571–573. https://doi.org/10.1038/41534 (1997).
17. Zhang, Y.-G. & Guo, G.-J. Molecular dynamics calculation of the bulk viscosity of liquid iron–nickel alloy and the mechanisms for the bulk attenuation of seismic waves in the Earth's outer core. *Phys. Earth Planet. Inter.* **122**, 289–298 (2000).
18. de Wijs, G. A. *et al.* The viscosity of liquid iron at the physical conditions of the Earth's core. *Nature* **392**, 805–807 (1998).
19. Cao, Q.-L. & Wang, P.-P. Stokes-Einstein relation in liquid iron-nickel alloy up to 300 GPa. *J. Geophys. Res. Solid Earth* **122**, 3351–3363. https://doi.org/10.1002/2016jb013878 (2017).
20. Schoen, M. & Hoheisel, C. The mutual diffusion coefficient D12 in binary liquid model mixtures. Molecular dynamics calculations based on Lennard-Jones (12–6) potentials: I. The method of determination. *Mol. Phys.* **52**, 33–56 (1984).
21. Liu, X. *et al.* Fick diffusion coefficients in ternary liquid systems from equilibrium molecular dynamics simulations. *Ind. Eng. Chem. Res.* **51**, 10247–10258 (2012).

22. White, A. J., Ticknor, C., Meyer, E. R., Kress, J. D. & Collins, L. A. Multicomponent mutual diffusion in the warm, dense matter regime. *Phys. Rev. E* **100**, 033213. https://doi.org/10.1103/PhysRevE.100.033213 (2019).
23. Zwanzig, R. & Ailawadi, N. K. Statistical error due to finite time averaging in computer experiments. *Phys. Rev.* **182**, 280 (1969).
24. Kresse, G. & Hafner, J. Ab initio molecular dynamics for liquid metals. *Phys. Rev. B* **47**, 558 (1993).
25. Kresse, G. & Furthmüller, J. Efficient iterative schemes for ab initio total-energy calculations using a plane-wave basis set. *Phys. Rev. B* **54**, 11169 (1996).
26. Blöchl, P. E. Projector augmented-wave method. *Phys. Rev. B* **50**, 17953 (1994).
27. Kresse, G. & Joubert, D. From ultrasoft pseudopotentials to the projector augmented-wave method. *Phys. Rev. B* **59**, 1758 (1999).
28. Perdew, J. P., Burke, K. & Ernzerhof, M. Generalized gradient approximation made simple. *Phys. Rev. Lett.* **77**, 3865 (1996).
29. Mermin, N. D. Thermal properties of the inhomogeneous electron gas. *Phys. Rev.* **137**, A1441 (1965).
30. Labrosse, S., Poirier, J.-P. & Le Mouël, J.-L. The age of the inner core. *Earth Planet. Sci. Lett.* **190**, 111–123 (2001).
31. Alfe, D. & Gillan, M. J. First-principles calculation of transport coefficients. *Phys. Rev. Lett.* **81**, 5161 (1998).

Acknowledgements

Author contributions

W.-J.L. designed and planned the project of this research. C.W., Z.L., P.Z., Y.L., Z.M., Q.J., X.-B.C., and H.-D.H. discussed the interpretation of the calculation results. All authors contributed to the preparation the manuscript and have approved the submitted version of the manuscript.

Competing interests

The authors declare no competing interests.

Additional information

Correspondence and requests for materials should be addressed to W.-J.L. or C.W.

Reprints and permissions information is available at www.nature.com/reprints.

Publisher's note Springer Nature remains neutral with regard to jurisdictional claims in published maps and institutional affiliations.